THE JOURNAL OF PHYSICAL CHEMISTRY B

Article

pubs.acs.org/JPCB

How Cholesterol Tilt Modulates the Mechanical Properties of Saturated and Unsaturated Lipid Membranes

George Khelashvili[†,*] and Daniel Harries[‡,*]

[†]Department of Physiology and Biophysics, Weill Cornell Medical College, New York, New York 10065, United States

[‡]Institute of Chemistry and the Fritz Haber Research Center, The Hebrew University of Jerusalem, Jerusalem 91904, Israel

ABSTRACT: Although there have been great advances in understanding the effect of cholesterol on various properties of lipid membranes, its mechanistic role in determining the elasticity of bilayers at the molecular level is not fully resolved. Indeed, to date the molecular mechanisms that drive the experimentally detected differences in properties of saturated and unsaturated lipid bilayers that contain cholesterol remain unclear. By quantifying the cholesterol orientational degrees of freedom from atomistic molecular dynamics simulations of mixed lipid-cholesterol membranes, we address this question from the perspective of cholesterol tilt and splay. Following the fluctuations in orientations of cholesterol and of lipid molecules in simulations, we have extracted tilt and splay moduli both for cholesterol molecules and hydrocarbon lipid tails. This has further allowed us to estimate the contributions of these modes to the response of membranes to elastic deformations. We find that tilt and splay deformations importantly contribute to the overall elasticity of the mixed lipid membranes, and that they can account for the experimentally established differences between the liquid ordered sphingomyelin (SM)/cholesterol bilayers and fluid dioleoylphosphocholine (DOPC)/cholesterol bilayers. These findings underscore the importance of tilt and splay moduli, derived from simulations with relative computational ease, as useful metrics for quantitatively characterizing the mechanical properties of mixed lipid-cholesterol bilayers.

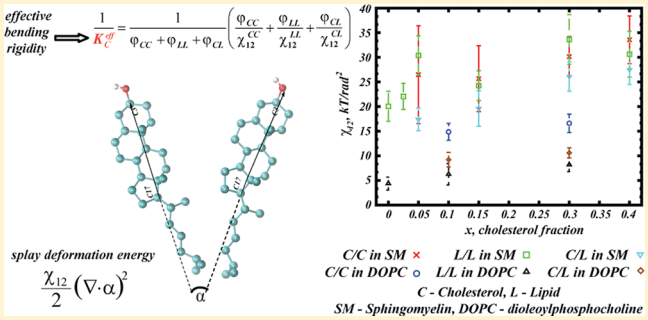

INTRODUCTION

Because cholesterol is vital for the proper function of eukaryotic plasma membranes, the way it affects the structural, thermodynamic, and mechanical properties of cholesterol-containing lipid bilayers has long been extensively studied (see ref 1−7 and citations therein). These explorations have established that cholesterol (Chol) more strongly influences saturated phosphocholine lipids (PCs) than it does unsaturated PCs.[1,2] These differential effects are manifested in several ways. For example, when added to saturated PC membranes, Chol induces substantial bilayer thickening concurrent with a decrease in the area per lipid molecule.[8−22] This thickening results from a Chol-induced straightening of lipid hydrocarbon tails in the direction normal to the membrane plane.[23] This "condensing effect" of cholesterol[18,24,25] is significantly less pronounced with lipid bilayers composed of unsaturated lipids. Indeed, X-ray diffraction measurements[1,2] reveal that the addition of 30% Chol increases membrane thickness (calculated as the phosphate-to-phosphate distance between the two leaflets) by a factor of ∼1.2 (5 Å) in saturated DMPC (dimyristoylphosphatidylcholine) lipid membranes, but only ∼1.1-fold (∼3 Å) in monounsaturated DOPC (dioleoylphosphocholine) lipid bilayers. On the macroscopic level, the stronger condensation of cholesterol on saturated lipids has been interpreted in terms of a unique Chol-specific thermodynamic state of fluidity, termed the liquid ordered (L_o) phase.[26,27] In the L_o phase lipid diffusion is comparable to that in the high-temperature fluid (L_α) phase, but in contrast the bilayer is thicker, as in low temperature gel phase membranes, resulting in straight, ordered hydrocarbon lipid chains.[26−28]

The differential cholesterol effects on saturated versus unsaturated lipids are perhaps even more striking when considering changes in the mechanical properties of these bilayers. Thus, experiments have established that the addition of up to 40% Chol does not change the bending rigidity, K_C, of membranes composed of DOPC lipids, whereas similar amounts of cholesterol increase K_C for DMPC lipid bilayers by about 5-fold to a value of $\sim 35 k_B T$ (per monolayer).[1] Similarly, high bending constants were measured in membranes containing 18:0/18:1 sphingomyelin (SM) lipid mixed with 30−50% Chol.[29] Possessing properties that are similar to those of typical saturated phosphoilipids, SM is of particular interest to cell physiology because SM/Chol complexes have been implicated in formation of functional microdomains, or "rafts", across plasma membranes (see, for example, refs 30−34 and citations therein).

Received: December 11, 2012
Revised: January 16, 2013
Published: January 16, 2013

   dx.doi.org/10.1021/jp3122006 | J. Phys. Chem. B 2013, 117, 2411−2421

What are the molecular mechanisms that drive the observed differences in properties of saturated and unsaturated lipid bilayers containing cholesterol? Although from the structural and thermodynamic perspectives this question has been addressed comprehensively using both biophysical experiments and computational simulations, a quantitative understanding of the molecular underpinnings of the mechanical (elastic) properties of Chol-containing mixtures is still lacking.

Major contributions to the elastic properties of lipid membranes have been associated with the ability of lipids to tilt with respect to the membrane normal direction (lipid tilt deformation) or to change their orientation with respect to each other (lipid splay deformation).[35−37] Moreover, it has been shown that the presence of cholesterol in lipid membranes dramatically affects these deformation modes. These studies suggested that Chol differently modulates the tilting of unsaturated and saturated lipids.[11] Indeed, the presence of cholesterol was found to largely increase the probability of saturated lipid tails to orient close to the membrane normal, whereas the orientation of unsaturated lipids remains broadly distributed.[11,19] Remarkably, this differential effect of cholesterol on lipids of different degrees of saturation appears to stem from the propensity of Chol molecules themselves to reorient in these bilayers. Indeed, in the presence of poly unsaturated fatty acids (PUFAs),[38] or even of short-chain monounsaturated diC14:1 PC lipid,[39] cholesterol with its hydroxyl group can lie deep inside the hydrocarbon core of the lipid bilayer. Furthermore, molecular dynamics (MD) simulations[19] of saturated DMPC lipid and Chol with different Chol content revealed that the tendency for cholesterol to tilt in the lipid membranes is concentration-dependent. For low sterol concentrations (<10%) a significant probability was found for Chol molecules to "lie down" in DMPC membranes. This tendency gradually diminished with increasing Chol fraction, and at high concentrations (>30%), cholesterol molecules were more strongly aligned with the normal to the bilayer plane.

To describe in rigorous, quantitative terms the mechanisms of lipid chain tilting in Chol-containing membranes and, with that, to gain molecular level understanding of how cholesterol modulates the elastic properties of lipid membranes, we use MD simulations. We use these simulations to obtain moduli for lipid tilt and splay deformations, which describe the corresponding free energy costs associated with lipid tilt and splay in mixed lipid/cholesterol bilayers. We make use of a recently reported, novel formulation to derive the cholesterol tilt modulus, χ_{CHOL}, from relatively small-scale unbiased atomistic MD simulations.[19,40−42] This modulus serves as a quantitative measure of the energetic cost of tilting cholesterol molecules inside the lipid membrane. Specifically, for DMPC/Chol mixtures, we showed how χ_{CHOL} can be derived from the sterol tilt probability distributions and demonstrated that χ_{CHOL} conveniently characterizes the "condensing effect" of cholesterol on DMPC lipids. With that, χ_{CHOL} can be used to link structural and thermodynamic properties of cholesterol-containing lipid membranes.

In the current work, we have extended this formalism in several new ways to extract the tilt and splay moduli from MD simulations. We explored the changes in cholesterol tilt modulus χ_{CHOL} in lipid membranes consisting of Chol mixed with either saturated lipid (SM) or unsaturated lipid (DOPC). By considering a wide range of cholesterol concentrations, we find that χ_{CHOL} is substantially higher (2−3 fold) in liquid-ordered membranes compared to fluid bilayers. Furthermore, we used MD simulations to derive the tilt modulus χ_{LIP} for lipid chains, using a similar procedure based on tilt angle distributions of lipid membranes. Interestingly, our analysis for SM/Chol bilayers revealed that χ_{LIP} and χ_{CHOL} are nearly identical for SM/Chol mixture in the liquid ordered state (i.e., for high cholesterol concentrations), but are different otherwise. Whereas both χ_{LIP} and χ_{CHOL} for DOPC/Chol complexes showed similar values, they were substantially lower than those measured for SM/Chol mixtures.

Importantly, we used the distribution of angles between pairs of cholesterols or pairs of lipid chains to calculate the splay moduli for cholesterol (χ_{12}^{CHOL}) and lipid chains (χ_{12}^{LIP}). Our results show that χ_{12}^{CHOL} and χ_{12}^{LIP} are nearly identical in liquid ordered membranes but are much different in bilayers of higher disorder (L_α phase).

We relate χ and χ_{12} for lipids and cholesterol obtained from the MD simulations to membrane tilt and splay deformation moduli, k_t and k_s, respectively. With that, our results establish a quantitative link between cholesterol organization inside lipid membranes (i.e., tilt) and the mechanical properties it induces in these membranes. Furthermore, we suggest that the tilt and splay parameters we obtained from MD simulations should be routinely used as necessary phenomenological constants in multiscaled simulations of lipid membrane models that help to relate the molecular and coarse-grained details.

COMPUTATIONAL METHODS AND PROCEDURES

Molecular Dynamics (MD) Simulations. Explicit solvent MD simulations were performed on 18:0/18:1 sphingomyelin (SM) lipid bilayers containing 0, 2.5, 5, 15, 30, and 40% cholesterol (Chol) number fractions, and on dioleoylphosphocholine (DOPC) lipid bilayers containing 0, 10, and 30% Chol number fractions (for complete specifications of simulated constructs see Table 1). For SM-containing membranes, the simulations were carried out at T = 50 °C, and for DOPC-containing bilayers, the simulations were run at T = 30 °C. All of the systems, therefore, were investigated above the gel-to-fluid transition temperatures of the respective pure lipid constituents.[43,44]

Table 1. Lipid Complexes Studied with MD Simulations[a]

lipid type	N_{LIPID}	N_{CHOL}	N_w	T, °C	time, ns
SM	400	0	12 648	50	40
SM	390	10	12 648	50	40
SM	380	20	12 648	50	40
SM	340	60	12 648	50	40
SM	280	120	12 648	50	40
SM	240	160	12 780	50	40
DOPC	512	0	19 300	30	40
DOPC	464	48	19 300	30	40
DOPC	360	152	19 300	30	40

[a] N_{LIPID}, N_{CHOL}, and N_w denote number of lipids (either SM or DOPC), cholesterol and water molecules in mixtures respectively.

To design mixtures of appropriate lipid/cholesterol compositions, we used hydrated membrane bilayer patches of pure SM (100 lipids) and pure DOPC (128 lipids) that were equilibrated with the Gromacs software,[45] using the recently improved 43A1-S3 lipid united atom force field.[46] This parameter set, used for all MD simulations reported in the current work, was described in detail in ref 46 and has been successfully tested for various lipid membrane systems, including different lipid/

dx.doi.org/10.1021/jp3122006 | J. Phys. Chem. B 2013, 117, 2411−2421

cholesterol mixtures, and has been shown for many lipid bilayers to yield structural characteristics that are in close quantitative agreement with those obtained from experimental models.

The original SM and DOPC patches were replicated 4 times in the membrane plane, *xy* directions, and appropriate cholesterol concentrations were created by randomly replacing a suitable number of lipids by cholesterol molecules. Table 1 lists full details of the simulated mixtures.

The simulations were carried out using the LINCS algorithm to constrain all bond lengths[47] allowing for 2 fs time steps. Periodic boundary conditions were applied in all three dimensions, and long-range electrostatics were calculated using the PME algorithm.[48] A cutoff of 18 Å was employed for van der Waals interactions. The systems were simulated in the *NPT* ensemble. A constant pressure of 1 atm was maintained using the Parrinello-Rahman semi-isotropic pressure coupling scheme,[49,50] and constant temperature was maintained using the Nosé-Hoover temperature coupling method.[51]

Calculation of Cholesterol and Lipid Tilt Modulus from MD Simulations. We have previously described the procedure for calculating the cholesterol tilt modulus χ from MD simulations.[19] Here, we use the same framework to obtain the moduli χ_{CHOL}, χ_{SM}, and χ_{DOPC} for Chol, SM, and DOPC lipids, respectively, in the SM-Chol and DOPC-Chol membranes. Briefly, the tilt angle, θ, was defined in the range $[0°; 90°]$ as the polar angle between the vector *t*, defining the director of lipid or Chol and the normal to the membrane plane. For Chol, *t* joins C3−C17 (see Figure 1), commonly used to describe the sterol ring plane orientation and the bilayer normal.[19] In this definition, $\theta = 0$ represents a sterol orientation where the ring plane is parallel to the bilayer normal (*z* axis). The lipid chain tilt angle was defined as the polar angle between the vector joining two methylene carbons in the hydrocarbon lipid chain, best representing the overall orientation of the chain (see also Results and Figure 2) and the bilayer normal. Since lipid tails are highly flexible, we chose to represent each chain of SM and DOPC lipid with two such vectors. For SM acyl chain (Figure 1), the carbon pairs selected were C21−C30 and C21−C31; for SM sphingosine chain, C41−C48 and C41−C49; for *sn-1* chain on DOPC, C19−C29 and C19−C30; and for *sn-2* chain on DOPC, C40−C50 and C40−C51. Orientational angle histograms of these vectors (4 vectors in total per lipid) were created, and normalized probability densities for SM and DOPC lipid tails were subsequently constructed.

Then, the normalized probability density $P(\theta)$ of the sterol or lipid tilt angle with respect to the bilayer normal was constructed for each simulated system. The $P(\theta)$ distribution was obtained by creating a sterol orientational angle histogram in the angular range $[0°; 90°]$. To calculate the sterol tilt modulus, a quadratic fit was performed to an expression of the form $-k_BT \ln[P(\theta)/\sin\theta]$ over the small angle range chosen to represent the best-sampled angular region and at the same time to limit the fit to the low θ regime where the quadratic expansion of the free energy with respect to tilt is most valid (see the Results section).[19,52] Finally, χ was determined from the coefficient that corresponded to the best fit. We note that a somewhat different choice of lipid tail directional vectors resulted in tilt moduli values that were within the error bars shown in Figure 6.

Calculation of Cholesterol and Lipid Splay Moduli from MD Simulations. Using the same director vector definitions as above for Chol, SM, and DOPC lipid tails, we calculated the cholesterol and lipid tail splay moduli, χ_{12}, from the normalized distributions of angles between pairs of cholesterol molecules and lipid tail pairs, respectively. Specifically, to obtain χ_{12}^{CHOL} for cholesterol, we constructed the normalized probability density $P_{12}(\alpha)$ of the angles α between ring planes of two Chol molecules by creating an angular histogram that included all Chol pairs within 10 Å from each other, a cutoff distance that was based on details of cholesterol ordering (see the Results section). The distance was measured as the separation between oxygen atoms on two Chol molecules, see the Results section, but was not sensitive to this choice of reference. The histogram included only those Chol pairs for which at least one of the cholesterol molecules was tilted by an angle of no more than $\theta = 10°$ with respect to the bilayer normal, representing small perturbations that are justified by the quadratic expansion of the free energy in θ (see the Results section and Figure 7). To calculate χ_{12}^{CHOL}, a quadratic fit was performed to $-k_BT \ln[P_{12}(\alpha)/\sin\alpha]$ over the small α angle range, and χ_{12}^{CHOL} was determined from the coefficient that corresponded to the best fit.

For SM and DOPC, χ_{12}^{SM} and χ_{12}^{DOPC} splay moduli were obtained in a similar manner, by constructing normalized probability densities of angles between pairs of C21−C30 (for SM) and C19−C29 (for DOPC) vectors. Here, as well, only tail pairs within 10 Å from each other (a distance measured as the separation of carbonyl carbons on two lipid chains) were considered, and the analysis took into consideration only those tail pairs for which at least one of the chains was tilted by no more than $\theta = 10°$ with respect to the bilayer normal.

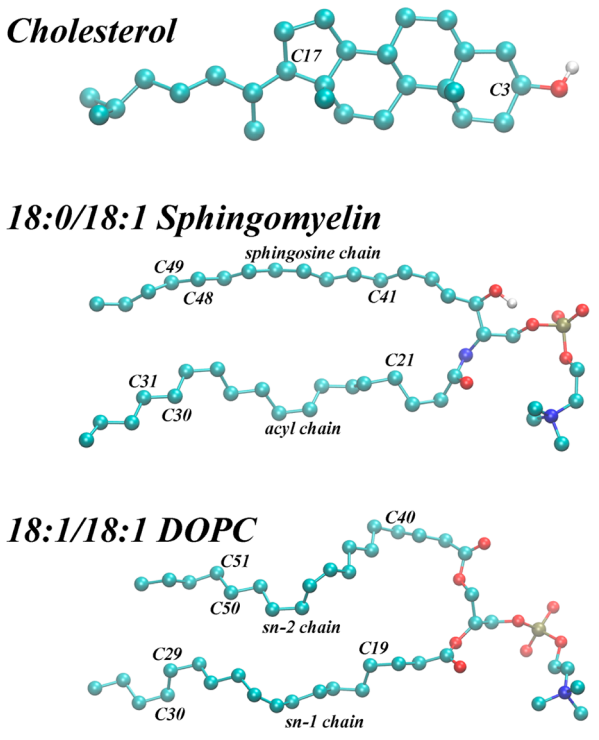

Figure 1. Ball-and-stick representation of cholesterol, 18:0/18:1 sphingomyelin (SM), and 18:0/18:0 1,2-dioleoyl-*sn*-glycero-3-phosphocholine (DOPC) molecules. The key atoms used for calculation of tilt distributions (see text) are labeled.

dx.doi.org/10.1021/jp3122006 | J. Phys. Chem. B 2013, 117, 2411−2421

For each fitting procedure, the quality of the fit was assessed by the reduced chi-squared parameter, which typically was found to be low, 10^{-3}–10^{-4}, signifying the good quality of the fit.

RESULTS

To study the effects of cholesterol on structural and mechanical properties of lipid bilayers in raft-like liquid ordered (L_o) and fluid (L_α) liquid disordered environments, using explicit-solvent atomistic MD simulations, we investigated mixed lipid membranes composed of Chol with 18:0/18:1 sphingomyelin (SM) lipid (the predominant sphingolipid in bovine brain[43]) or with 18:1/18:1 dioleoylphosphocholine (DOPC) lipid. A broad range of Chol concentrations were explored: 0–40% for SM/Chol and 0–30% for DOPC/Chol (Table 1). For SM/Chol mixtures at 50 °C, the experimentally determined temperature–composition diagram predicts formation of L_o phase already for 7 ± 2% Chol.[43] The L_o phase is expected to coexist with the fluid L_α phase for up to 25 ± 5% Chol content. For mixtures with more than 30% Chol, only a single, uniform L_o phase exists.[43] For DOPC/Chol binary complexes at 30 °C, experiments show that the fluid phase is maintained throughout the cholesterol concentration range studied here.[1,53]

Lipid Tail Ordering in SM/Chol and DOPC/Chol Bilayer Mixtures. To quantify the molecular level organization in SM/Chol and SM/DOPC membranes, we first calculated from MD the equivalent of the lipid tail deuterium order parameters ($-S_{CD}$).[14] Figure 2 shows trends in $-S_{CD}$ for the acyl chain of SM lipid and for the (unsaturated) tails of the DOPC lipid.

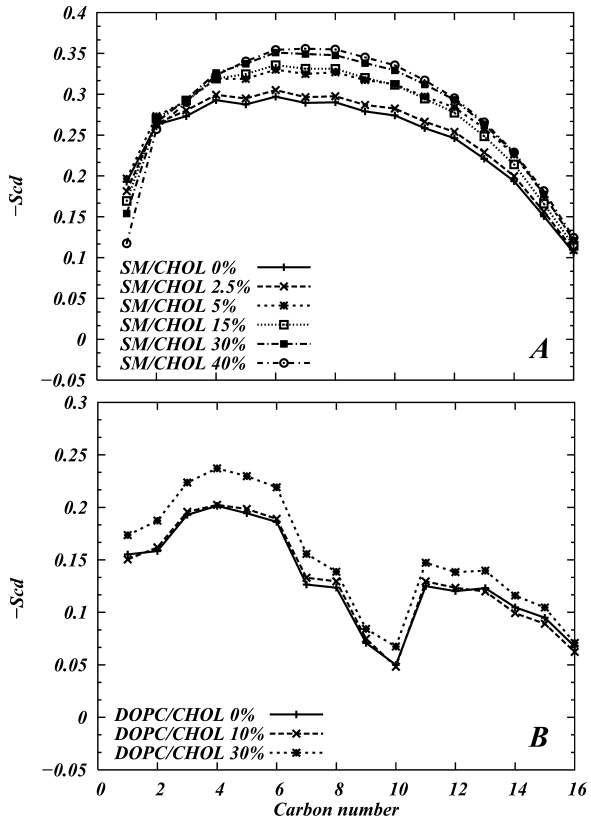

Figure 2. Deuterium order parameter ($-S_{CD}$) profiles derived from simulations. $-S_{CD}$ for SM acyl chain (A) and $-S_{CD}$ averaged over two chains of DOPC lipid (B) are shown at different cholesterol concentrations.

$-S_{CD}$ is a measure of the average lipid tail orientation along the axis normal to the membrane plane and is directly related to bilayer thickness.[1] In simulations that use the united atom force field, $-S_{CD}$ for saturated and unsaturated methylene carbons in the lipid tail can be determined using the following relations:[14]

$$-S_{CD}^{SAT} = \frac{2}{3}S_{xx} + \frac{1}{3}S_{yy} \quad (1)$$

and

$$-S_{CD}^{UNSAT} = \frac{1}{4}S_{zz} + \frac{3}{4}S_{yy} \mp \frac{\sqrt{3}}{2}S_{yz} \quad (2)$$

respectively. In the above, "∓" refers to the two carbons that form the unsaturated bond, and S_{ij} are the components of the order parameter tensor:

$$S_{ij} = \frac{1}{2}\langle 3\cos\beta_i \cos\beta_j - \delta_{ij}\rangle, \quad i, j = x, y, z \quad (3)$$

where β_i is the angle formed between the ith molecular axis with the bilayer normal and δij represents the Kronecker delta function.

Consistent with the established phase behavior of SM/Chol mixtures, Figure 2A reveals that at 50 °C the ordering of the hydrocarbon chains of SM lipid strongly increases with cholesterol content and saturates at ∼30% cholesterol. In fact, in line with the experimental temperature–composition phase diagram for SM/Chol systems,[43] our data suggests that the Chol-induced liquid ordered (L_o) state in SM bilayers sets in at 5% sterol concentration (witnessed as the region where $-S_{CD}$ values experience a large increase between 2.5% and 5%, Figure 2A) and coexists with the fluid (L_α) state up to 30% Chol (seen as $-S_{CD}$ in Figure 2A that is similar for 5% and 15% but increases significantly between 15% and 30% Chol). Finally, from 30% upward, only the L_o state remains, as SM chain order parameters do not vary between 30% and 40% Chol (Figure 2A).

For DOPC/Chol mixtures at 30 °C, Figure 2B suggests that the overall magnitude of the lipid tail order parameter change upon addition of 30% Chol is about half of that in SM/CHOL membranes. This finding is also in accordance with the experimental evidence (see for example, ref 1) that suggests that cholesterol's influence on ordering of unsaturated lipids such as DOPC is much weaker than it is on saturated lipids. Furthermore, Figure 2B shows the characteristic drop in order parameter at the unsaturated bond (between carbons C9 and C10) in the DOPC chains. Taken together, the data presented in Figure 2 suggests that organization of lipid tails in our simulated bilayers are in line with that expected from experimental observations.

Organization of Cholesterol and Lipid Tails in SM/Chol and DOPC/Chol Bilayers. *Cholesterol Tilt and Lipid Tail Tilt Are Related.* To examine how the organization of SM and DOPC lipid tails is influenced by cholesterol, we followed the tilt angles of hydrocarbon chains of SM and DOPC lipids and of cholesterol molecules in the MD simulations. Figure 3A shows the normalized probability density distributions $P(\theta)$ of Chol tilt angle θ in SM/Chol membranes and Figure 3C depicts those in DOPC/Chol bilayers.

The distribution plots for SM/Chol mixtures show the trends established previously for mixtures of cholesterol with saturated lipids:[9,19,41,54–56] At low concentrations (<5%), cholesterol molecules tend to tilt with respect to the bilayer normal, as $P(\theta)$ distributions are relatively broad (see SM/Chol 5% in

dx.doi.org/10.1021/jp3122006 | J. Phys. Chem. B 2013, 117, 2411–2421

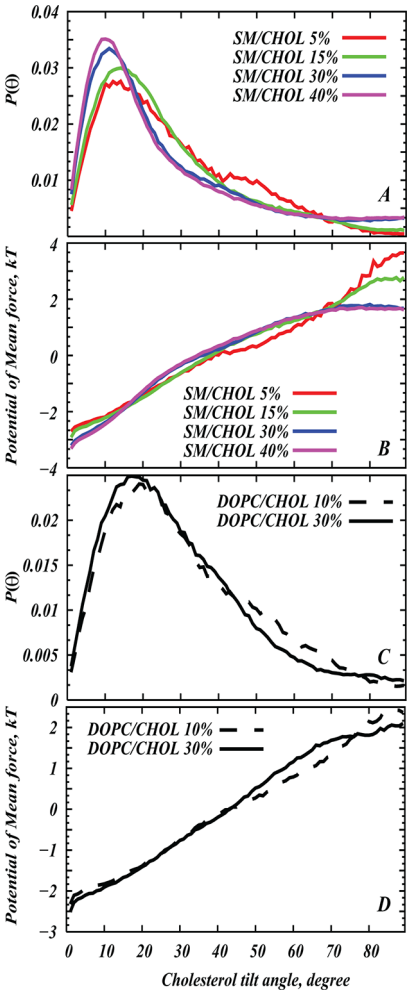

Figure 3. Normalized probability distributions of cholesterol tilt angle, $P(\theta)$, in SM/Chol (A) and in DOPC/Chol (C) membranes for various cholesterol concentrations (see the Methods section for details). Panels B and D show the potential of mean force (PMF) plots derived from the distributions in panels A and C, respectively (see text for details). The color codes for panels A and B and for panels C and D are the same.

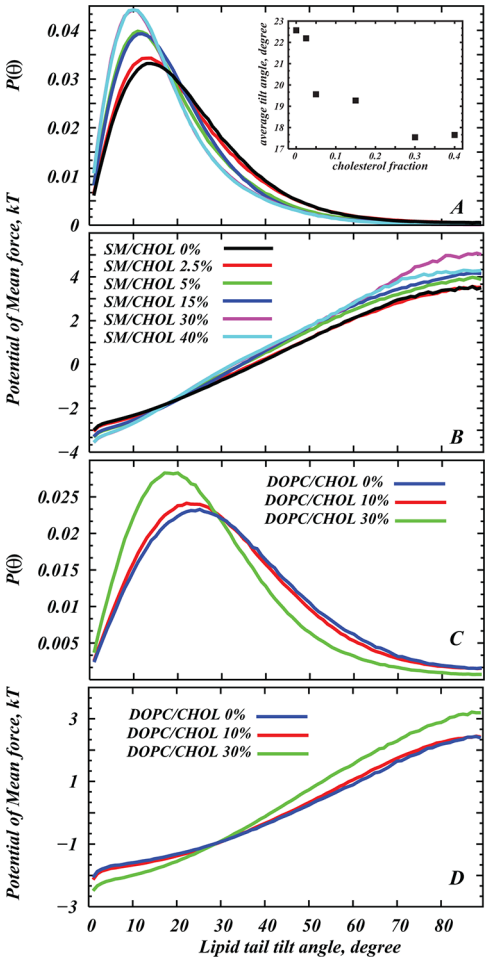

Figure 4. Normalized probability distributions $P(\theta)$ of SM acyl chain tilt angle in SM/Chol membranes (A) and of DOPC *sn-1* chain in DOPC/Chol bilayers (C) for various cholesterol concentrations (see the Methods section for details). The inset in panel A shows the dependence of average SM acyl chain tilt on cholesterol concentration. Panels B and D show the potential of mean force (PMF) derived from the distributions in panels A and C, respectively (see text for details). The color codes for panels A and B and for panels C and D are the same.

Figure 3A). Upon increasing concentration, Chol molecules in SM membranes undergo a transition from "lying down" to "standing up" states, as $P(\theta)$, shown in Figure 3A, progressively develops a well-defined narrow peak at lower θ angles. Notwithstanding, even at high Chol concentrations, some fraction of cholesterol molecules can still be found oriented perpendicular to the membrane normal (seen as a nonzero probability for high θ in SM/Chol mixtures at 30% and 40% Chol). At the highest values of the tilt angle the probability $P(\theta)$ is close to zero for intermediate cholesterol concentrations (5 and 15%), probably due to poor statistics of cholesterol orientations at these fractions and high angles.

Comparison of $P(\theta)$ profiles obtained for Chol in SM (Figure 3A) and DOPC (Figure 3C) membranes reveals that in unsaturated DOPC bilayers, the most probable tilt angle of cholesterol is found at higher θ value. Indeed, at 30% Chol, for example, the peak in $P(\theta)$ measured in SM/Chol membranes is at ~10°, whereas in DOPC/Chol the most probable angle for Chol tilt is ~16°.

Differential tilt of cholesterol in SM and DOPC membranes corresponds to distinct tilting of lipid tails. Thus, Figure 4, panels A and C, compares orientations of SM and DOPC lipid chains in the simulations. Consistent with the order parameter data (Figure 2A) and with the tilt distribution plots for cholesterol molecules (Figure 3), Figure 4A shows a gradual alignment of SM tails along the membrane normal as cholesterol concentration increases. The average tilt angle of SM chains (Figure 4A inset) appears to exhibit three distinct populations when plotted against Chol fraction, consistent with the trends in SM tail order parameters (see Figure 2). Although in MD simulations of finite-size membrane patches phase coexistence is hardly captured, the three distinct populations can be attributed to the formation of the L_o state at ~5% Chol, which remains in coexistence with the fluid L_α state up to 30% Chol, where the disordered phase completely disappears. Taken together, the tilt distribution profiles of Chol and SM lipid tails suggests that orientation of cholesterol molecules and SM chains are correlated.

Similar correlation can be observed between the tilt of Chols and hydrocarbon tails of DOPC lipids (Figures 3C and 4C). However, in contrast to SM lipids, DOPC lipid chains remain

dx.doi.org/10.1021/jp3122006 | J. Phys. Chem. B 2013, 117, 2411−2421

relatively tilted with respect to membrane normal even at high Chol fractions (compare panels C and A in Figure 4), consistent with the observation that cholesterol molecules are more aligned with respect to the bilayer axis in SM membranes compared with DOPC bilayers.

Long-Range Ordering of Cholesterol Molecules Is Different in SM and DOPC Bilayers. Differential alignment of cholesterol in SM and DOPC bilayers could also result in distinct long-range orientational order for Chol molecules in the two membranes. We have shown previously that the existence of such long-range organization is generally important because it relates to the strong aligning field cholesterol creates in lipid membranes.[19,40,41] To quantify this Chol ordering, we calculated the cholesterol orientational order parameter, σ, using the definition[57]

$$\sigma = \left\langle \frac{1}{2}(3\cos^2\alpha - 1) \right\rangle \tag{4}$$

In the above, α denotes the angle between the vectors defining the ring plane direction of two cholesterols (see the Methods section); $\sigma = 1$ if Chols are perfectly aligned, and $\sigma = 0$ for the orientationally isotropic mixture. In Figure 5, we show σ as a function of the distance between cholesterol pairs for SM/Chol and DOPC/Chol mixtures. Because packing of cholesterol around SM and DOPC lipid is expected to be different (see for example refs 58 and 22), the corresponding peak separations in the σ plots in Figure 5, representing neighboring shells, differ as well. As expected, the plots illustrate that cholesterol orientational order in the first neighboring shell, up to about 10 Å, increases with increasing Chol concentration; moreover, for high Chol fractions orientational ordering of Chol molecules generally persists over large distances. However, a comparison of panels A and B in Figure 5 also indicates stronger alignment of cholesterol molecules in SM/Chol bilayers compared to that in DOPC/Chol membranes. For example, at 30% Chol, σ is higher in SM/Chol than in DOPC/Chol mixtures, even for Chol pairs that are far apart (compare bulk values in Figure 5).

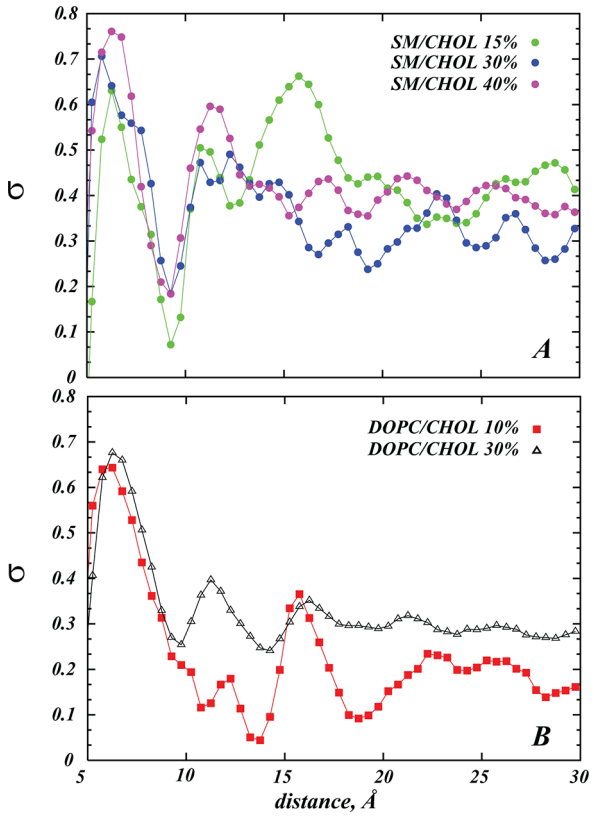

Figure 5. Cholesterol orientational order parameter σ (see text) as a function of distance between cholesterols. Results for 15, 30, and 40% SM/Chol systems (A) and for 10% and 30% DOPC/Chol mixtures (B) are shown as different symbols; lines represent guides to the eye.

It is also important to note the differences in σ measured in SM/Chol and DOPC/Chol bilayers, specifically for separations less than 10 Å, representing interactions between a Chol molecule and its immediate neighbors. In this first shell, increases in Chol composition has a significant impact on Chol alignment in SM membranes (σ increases with Chol content in Figure 5A), but in DOPC bilayers the effect is minor (from Figure 5B, σ in the first shell is similar in the 10% and 30% DOPC/Chol mixtures).

Tilt Moduli of Cholesterol and Lipid Tails. The aligning field created by cholesterol in SM and DOPC bilayers is significantly different, as evidenced in Figure 5. To quantify this effect, we have recently developed a formulation[19] that allows us to evaluate the cholesterol tilt modulus χ, an empirical parameter that serves as a measure of the force associated with tilting a sterol molecule inside a lipid membrane. As detailed elsewhere,[19,40,41] χ represents the coefficient of the quadratic term in the expansion of the transfer free energy of cholesterol from the aqueous medium into a lipid bilayer at an angle θ.

To obtained the cholesterol tilt modulus in SM and DOPC membranes from MD simulations, we make use of $P(\theta)$, the tilt angle probability distributions, shown in Figures 3A and 3C. These distributions can be used to define a potential of mean force (PMF) which in turn is used to extract the sterol tilt modulus, χ.[19] Specifically, we define PMF as

$$\mathrm{PMF}(\theta) = -k_B T \ln \frac{P(\theta)}{P_0(\theta)} \tag{5}$$

In the above, $P_0(\theta) = \sin\theta$ is the normalization condition representing the tilt angle probability distribution along a preferred direction (in this case the membrane normal axis) for a hypothetical system of noninteracting, randomly oriented molecules (director vectors).[19]

Shown in Figure 3, panels B and D, for cholesterol in SM and DOPC bilayers, the PMF as defined in eq 5 is closely related to the desolvation free energy of Chol introduced by Kessel et al.[52] and measures the free energy associated with tilting a cholesterol molecule by a $\Delta\theta = \theta_1 - \theta_2$ angle, so that the free energy change in this process is $\Delta\mathrm{PMF}(\Delta\theta) = \mathrm{PMF}(\theta_1) - \mathrm{PMF}(\theta_2)$. Since the PMF profiles in Figure 3 obey a quadratic behavior for low tilt angles (see the Methods section), the tilt modulus χ_{CHOL} for cholesterol can be obtained by fitting a quadratic function to the PMF plots in Figure 3, panels B and D, for the low angle regime (see also ref 19). Similarly, the tilt moduli for SM (χ_{SM}) and DOPC (χ_{DOPC}) lipid tails can be derived from the same fitting routine to the PMF plots (Figure 4, panels B and D) obtained from the probability distributions of lipid tail tilt angles (Figure 4, panels A and C). The resulting values for χ_{CHOL}, χ_{SM}, and χ_{DOPC} at different Chol concentrations are summarized in Figure 6.

Similar to our previous findings for DMPC/Chol membranes,[19] in SM/Chol mixtures χ_{CHOL} is strongly dependent on cholesterol concentration and varies in step with the phase evolution of SM/Chol bilayers. Thus, χ_{CHOL} is relatively low in

dx.doi.org/10.1021/jp3122006 | J. Phys. Chem. B 2013, 117, 2411−2421

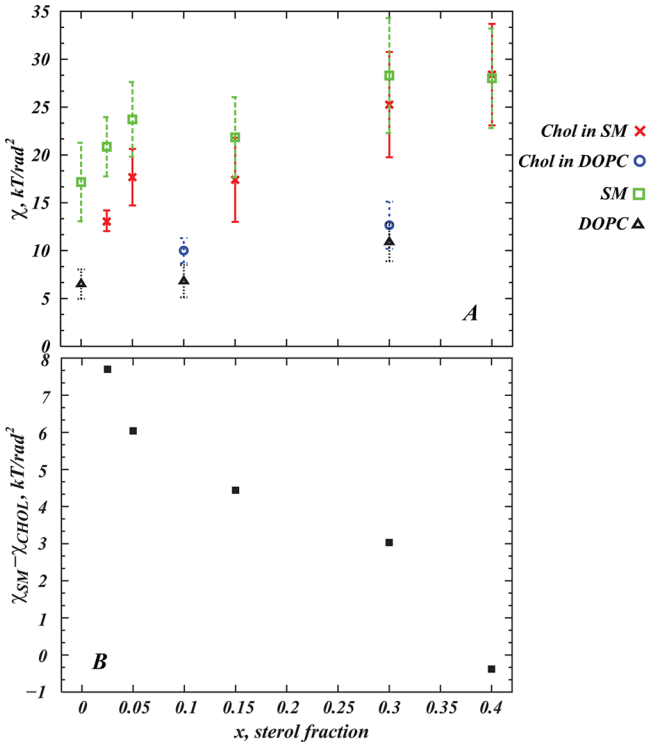

Figure 6. (A) Tilt modulus χ of cholesterol in SM (red crosses) and DOPC (blue circles) bilayers and tilt modulus of SM (green squares) and DOPC lipid tails (black triangles) in the respective bilayers as a function of sterol composition. For SM/Chol model membranes, χ for cholesterol and SM lipid tails were obtained by fitting quadratic function to the PMF plots in Figures 3B and 4B in the angular range of $\theta \in [5°; 20°]$. The error bars represent standard deviations from similar fits obtained over [5°; 10°], [10°; 15°], and [15°; 20°]. For DOPC/Chol model membranes, χ for cholesterol and DOPC lipid tails were derived by fitting a quadratic function to the PMF plots in Figures 3D and 4D in the angular range of $\theta \in [10°; 30°]$. Error bars represent standard deviations from similar fits taken over [10°; 17°], [17°; 24°], and [24°; 30°]. (B) The difference between the tilt modulus of SM and the tilt modulus of Chol, $\chi_{SM} - \chi_{CHOL}$, taken from panel A, as function of cholesterol concentration.

the fluid state (2.5% Chol) but progressively rises as the liquid ordered state become more prominent (χ_{CHOL} increases between 2.5% and 5%, and again between 15% and 30%), a trend that is consistent also with the variations in SM lipid tail order parameters (Figure 2A).

Interestingly, Figure 6A reveals that the cholesterol tilt modulus is different from the lipid tilt modulus χ_{SM} in the fluid L_α state. However, as the L_o phase sets in, the two moduli start to overlap (see the data for 5% and 15% Chol), and at the highest Chol concentrations (30−40%), χ_{SM} and χ_{CHOL} become very similar. The trend is even more evident when plotting the difference between the two moduli, Figure 6B. This correlation between χ_{SM} and χ_{CHOL} in the liquid ordered state suggests that the Chol-induced long-ranged alignment field arising in the L_o state (Figure 5A) strongly modulates the organization of SM lipid tails (see the Discussion section).

Remarkably, in DOPC/Chol membranes, even at high Chol compositions (30%), the tilt modulus for lipid tails (χ_{DOPC}) as well as for cholesterol molecules (Figure 6) remain significantly lower compared to the χ_{SM} and χ_{CHOL} tilt moduli measured in SM/Chol mixtures. This result is consistent with theoretical predictions on the exothermic nature of single Chol molecule transfer from the fluid phase to the liquid ordered phase membranes,[59] as well as on the free energy calculations of single Chol molecule desorption from membranes consisting of lipids with hydrocarbon tails of various levels of unsaturation.[60] In particular, all atom and coarse grained MD simulations predicted that the free energy of cholesterol desorption from saturated lipid bilayers was higher than that from membranes containing unsaturated lipids.[60] At the same time, the rate of cholesterol flip-flop was reduced with increasing lipid tail order. These trends are in agreement with our observations that the tilt modulus (for both Chol and lipid tails) remains low in the fluid phase but increases dramatically in the L_o state.

Splay Moduli of Cholesterol and Lipid Tails. It is informative to consider another property related to tilting of lipid and cholesterol molecules in lipid membranes, which we term the pair tilt modulus or splay modulus, χ_{12}. This modulus describes the tilting of one cholesterol or lipid molecule with respect to another. To calculate the splay modulus for cholesterol pairs (χ_{12}^{CHOL}), we derive the normalized density $P_{12}(\alpha)$ that describes the probability of finding two Chol molecules at an angle α between them (see the Methods section and also Figure 7A). Using a fitting procedure similar to that implemented for deriving the tilt modulus, we extracted from the PMF of $P_{12}(\alpha)$, shown in Figure 7B, the corresponding χ_{12}^{CHOL}, a measure that estimates the free energy penalty for splay, or more precisely, for tilting one sterol molecular director with respect to the other (see ref 41 for more details). In a similar manner, the lipid splay modulus (χ_{12}^{SM} or χ_{12}^{DOPC}, for SM and DOPC, respectively) was calculated from the $P_{12}(\alpha)$ for pairs of lipid tails (Figure 7, panels C and D). The resulting values for χ_{12} in different simulations are shown in Figure 8.

As for the tilt modulus, we find that also for the splay, the values for χ_{12}^{CHOL} and χ_{12}^{SM} are very similar in the liquid ordered state (see 5−40% SM/Chol data in Figure 8). Interestingly, the "cross" splay modulus, i.e., χ_{12} describing the splay between SM tails and cholesterol molecules, is somewhat lower than either χ_{12}^{CHOL} or χ_{12}^{SM} (Figure 8).

Remarkably, in the fluid state membranes (DOPC/Chol systems), our results suggest that not only are the splay moduli for both lipid tails and Chol molecules lower compared to those obtained in ordered SM/Chol membranes, but also that χ_{12}^{CHOL} and χ_{12}^{DOPC} are much different (Figure 8). In addition, we find that values of the "cross" splay modulus between cholesterol molecules and DOPC tails lie within the range of χ_{12}^{CHOL} and χ_{12}^{DOPC}. These results, together with the tilt moduli shown in Figure 6, suggest a fundamentally different effect of cholesterol tilt on organization of lipid molecules in ordered and disordered membranes.

DISCUSSION

Lipid tilt and splay deformation modes are considered as two of the major factors contributing to the elastic properties of lipid membranes.[35−37] Here, we explored quantitatively the distributions of instantaneous lipid tilt and splay in (on average) flat SM/Chol and DOPC/Chol membranes from atomistic MD simulations. We computed two thermodynamic parameters, the tilt modulus χ and the splay modulus χ_{12}, for cholesterol molecules and hydrocarbon tails of lipid molecules. The value of χ is directly related to the energy required to tilt a molecule with respect to the bilayer normal, and χ_{12} quantifies the free energy cost of tilting one molecule with respect to the other.

dx.doi.org/10.1021/jp3122006 | J. Phys. Chem. B 2013, 117, 2411−2421

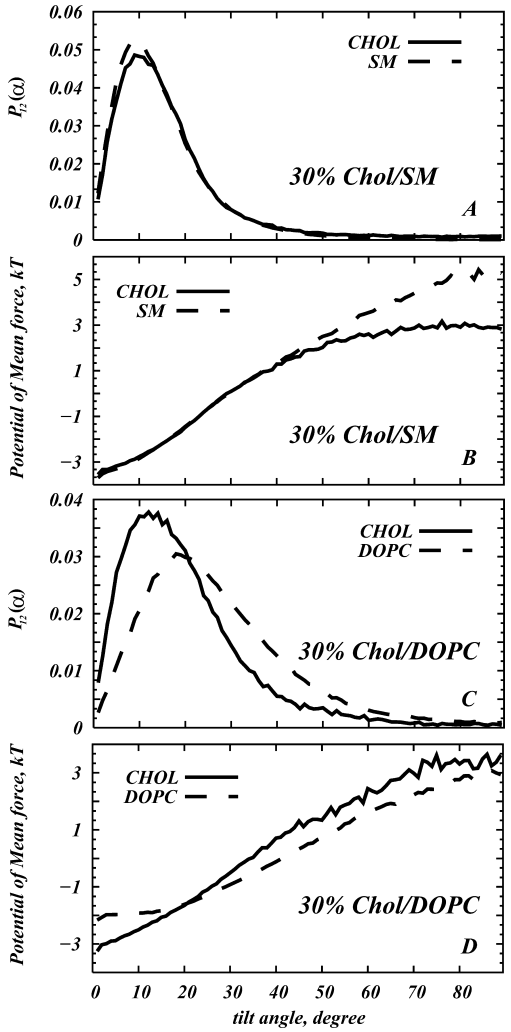

Figure 7. Normalized probability densities $P_{12}(\alpha)$ of finding pairs of sterol molecules (solid lines) or pairs of lipid tails (dashed lines) at an angle α with respect to each other (see the Methods section for definitions). The data is shown for 30% SM/Chol (panel A) and 30% DOPC/Chol (panel C) bilayers to allow a direct comparison. To limit the analysis to near neighbors, for these calculations, only molecules (pairs of Chol or lipid tails) within 10 Å distance of each other were included (see Figure 5 and the discussion in the text) from respective membranes, and consideration was given only to those pairs for which at least one of the molecules was tilted by an angle of no more than θ = 10° with respect to bilayer normal. Panels B and D depict respective potential of mean force profiles from which corresponding splay moduli χ_{12} were calculated (see Figure 8).

Comparing both χ and χ_{12} in fluid L_α membranes (DOPC/Chol) versus raft-like liquid ordered L_o bilayers (SM/Chol) affords several important insights. Specifically, the tilt moduli for SM lipid tails and cholesterol molecules are similar when that SM/Chol mixture has characteristics of the L_o state (for Chol compositions ≥5%), but they are different in fluid-like bilayers (for 2.5% Chol concentration). For DOPC/Chol mixtures that exhibit properties of the L_α state even at high Chol compositions, the tilt moduli for lipid tails and Chol molecules were similar but significantly lower compared to those obtained in ordered SM/Chol membranes. Remarkably, we also found that the splay modulus χ_{12} for lipid tails and Chol were similar in L_o membranes but different in L_α membranes.

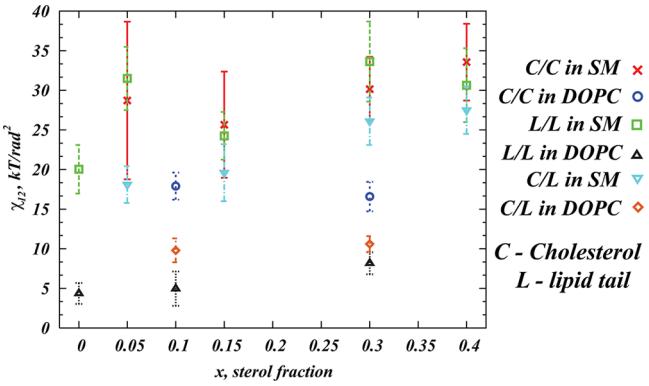

Figure 8. Splay modulus χ_{12} of cholesterol in SM (red crosses) and DOPC (blue circles) bilayers, of SM (green squares) and DOPC lipid tails (black triangles) in respective bilayers, and of cholesterol/SM lipid tail pairs (inverted cyan triangles) and cholesterol/DOPC lipid tail pairs (brown diamonds) as a function of sterol composition. For SM/Chol model membranes, χ_{12} moduli were obtained by fitting a quadratic function to the PMF plots in Figure 7, panels B and D, in the angular range of $\theta \in [5°; 20°]$. The error bars represent standard deviations from similar fits obtained over [5°; 10°], [10°; 15°], and [15°; 20°]. For DOPC/Chol model membranes, χ_{12} parameters were obtained by fitting quadratic function to the PMF plots in Figures 3D and 4D in the angular range of $\theta \in [10°; 30°]$. Error bars represent standard deviations from similar fits obtained over [10°; 17°], [17°; 24°], and [24°; 30°]. Note that, due to insufficient sampling of Chol pair interactions in 2.5% SM/Chol (Chols are too dispersed), we did not calculate χ_{12} for this mixture.

To establish a link between these findings and the experimentally observed differential effects of cholesterol on the mechanical properties of lipid bilayers consisting of saturated and unsaturated lipids,[29,61] we relate χ and χ_{12} parameters to phenomenological constants representing the response of membranes to deformations that require lipid tilt and splay. To learn about the membrane's response to an external deforming force, our strategy was to use the temporal lipid and sterol orientational fluctuations in simulations of membranes at equilibrium, which are flat on average. For small deformations, local changes in the average orientation of a molecule should come with a free energy penalty that can be determined from the relative probability of finding the same molecule in that orientation in an unperturbed membrane.

The energetic cost associated with membrane deformations can be evaluated using the theoretical approach to membrane elasticity[62−64] where each monolayer comprising a lipid bilayer is considered as a continuum, elastic medium, and is described by its local height, h, and by the local director, $\vec{t}$, that defines the average orientation of lipid chains.[35−37,65] The latter is given as

$$\vec{t} = \frac{\vec{n}}{\vec{n}\cdot\vec{N}} - \vec{N} \tag{6}$$

where $\vec{n}$ and $\vec{N}$ are the unit vectors along the lipid chain and membrane normal directions, respectively. The free energy describing deformations of each monolayer is then expressed to quadratic order in h and $\vec{t}$ as a sum of terms, representing the lipid tilt and splay contributions

$$f_{\text{tilt}} = \frac{k_t}{2}(\vec{t} - \nabla h)^2 \tag{7}$$

and

dx.doi.org/10.1021/jp3122006 | J. Phys. Chem. B 2013, 117, 2411−2421

$$f_{splay} = \frac{k_s}{2}(\nabla \cdot \vec{t})^2 \quad (8)$$

respectively. Here, f_{tilt} quantifies the resistance of the lipids in a membrane leaflet to tilt with respect to the membrane normal direction, and f_{splay} penalizes changes in lipid chain orientation. k_t and k_s in the above equations represent the tilt and splay moduli, respectively.

Since eqs 7 and 8 are strictly valid only in the limit of small tilt perturbations, it is straightforward to show that the mathematical formalism we developed to obtain χ and χ_{12} from MD relates to the same deformation modes described by eqs 7 and 8. Indeed, as demonstrated by several authors,[35−37] in the regime of small tilt angles, f_{tilt} and f_{splay} terms simplify to the expressions $(k_t/2)\theta^2$ and $(k_s/2)(\nabla\cdot\theta)^2$, respectively, with θ denoting the angle between the unit vectors along the membrane normal $\vec{N}$ and lipid tail director $\vec{n}$.

Therefore, the values for χ reported in Figure 6 represent contributions to k_t originating from the tilt of cholesterol molecules and lipid tails. From our analysis it then follows that f_{tilt} is higher for SM, as χ_{SM} is at least twice as large compared to χ_{DOPC} in Chol-free bilayers (Figure 6). This can partly be attributed to the ability of SM lipids to interdigitate between bilayer leaflets, as well as to engage in strong intra- and intermolecule hydrogen bonding (see refs 66−69 and citations therein). Our results, furthermore, suggest that f_{tilt} in SM bilayers increases even further upon addition of Chol and that it is higher by a factor of ∼2 in liquid ordered bilayers compared to the fluid membranes (Figure 6). Importantly, the presented data indicates that, in the L_o phase, energy penalties for tilting cholesterol molecules and lipid tails are similar (Figure 6B), suggesting that either χ_{SM} or χ_{CHOL} could serve for parametrization of k_t.

Remarkably, our findings in relation to the splay deformation mode (Figure 8) reveal that the energy cost of inducing a splay deformation between pairs of Chol molecules and pairs of lipid tails in L_o phase membranes are very similar (χ_{SM} and χ_{CHOL} parameters overlap in the range of 5−40% Chol concentrations, Figure 8), but in the more disordered, L_α phase bilayers the free energy required to tilt Chol molecules with respect to each other is larger than the cost of splay deformation between lipid tails (χ_{CHOL} in DOPC/Chol mixtures is ∼2−3 time larger than χ_{DOPC}).

These insights have direct implications for elastic properties of Chol-containing membranes. Indeed, when a membrane undergoes bending deformations, sterol and lipid molecules are forced to rearrange in the bilayer, and on average assume a more splayed configuration with respect to one another.[36] Therefore, splay deformations must contribute to the membrane bending energy. In fact, as noted in ref 36, the deformation modes stemming from lipid splay and membrane bending are analogous for lipid bilayers for which k_t is sufficiently large. Based on our tilt modulus data, this large k_t regime is consistent with the liquid ordered state of lipid membranes (30−40% SM/Chol) where tilt moduli for both lipid tails and cholesterol molecules reach high 25−30 k_BT/rad^2 values (Figure 6).

Interestingly, for lipid mixtures that are in the L_o state, we find that the energetic cost of splay deformations between pairs of lipid tails or pairs of cholesterol molecules (χ_{12} parameters) is also similar. To establish the significance of the χ_{12} splay moduli for bilayer bending deformations, we note that there have been several suggestions on how to average elastic properties of membranes that contain several different molecular components.[70−74] For example, Kozlov and Helfrich[71] introduced a simple model for two-component lipid bilayers, where the spontaneous curvature and the inverse bending modulus were expressed as a linear functions of the lipid composition. Safran et al.[70] related the effective spontaneous curvature in a given layer of two-surfactant mixtures to the probabilities of finding a pair of surfactant of type "1", of type "2", or of a mixed "1−2" pair. Based on these ideas, here we suggest a simple expression for the effective bending rigidity K_C^{eff} that weighs the contributions of the different χ_{12} moduli according to the probability of finding a lipid−lipid, sterol−lipid, or sterol−sterol pair in the mixture (as found in practice in the simulation)

$$\frac{1}{K_C^{eff}} = \frac{1}{\varphi_{CC} + \varphi_{LL} + \varphi_{CL}}\left(\frac{\varphi_{CC}}{\chi_{12}^{CC}} + \frac{\varphi_{LL}}{\chi_{12}^{LL}} + \frac{\varphi_{CL}}{\chi_{12}^{CL}}\right) \quad (9)$$

In the above, χ_{12}^{CC}, χ_{12}^{LL}, and χ_{12}^{CL} are the splay moduli for Chol/Chol, lipid tail/lipid tail, and Chol/lipid tail pairs, respectively, as obtained from the simulations (Figure 8), and φ_{CC}, φ_{LL}, and φ_{CL} denote numbers of corresponding nearest-neighbor pairs. The later measures were obtained directly from MD trajectories for each simulated mixture as number of Chol/Chol, lipid tail/lipid tail, and Chol/lipid tail pairs within 10 Å of each other (see the Methods section for more details). We note that, for all our simulations, the numbers for φ_{CC}, φ_{LL}, and φ_{CL} obtained in this manner were in close agreement with those expected for a randomly distributed mixture.

Monolayer bending rigidities for the simulated mixtures calculated according to eq 9 are listed in Table 2. As expected from the trends in the splay modulus parameter, K_C^{eff} is significantly larger for SM/Chol mixtures compared to DOPC/Chol systems. Importantly, the values we obtain from the simple relation in eq 9 are in good agreement with experimentally determined bending rigidities, K_C, for SM/Chol or DMPC/Chol complexes. Thus, using electrodeformation and fluctuation spectroscopy measurements, Gracià et al.[29] estimated K_C for SM/Chol mixture at 30−40% Chol and at 23 °C to be in the range of 45−60 k_BT. Using X-ray scattering, Nagle and co-workers[1,2] also found K_C for DMPC/Chol at 30% Chol and 30 °C to be high, reaching ∼33 k_BT. The same studies measured much lower bending rigidity (∼9−15 k_BT) for fluid DOPC/Chol bilayers at 30 °C. These values are consistent with the K_C^{eff} values detailed in Table 2 that were calculated for SM/Chol membranes at 50 °C and for DOPC/Chol mixtures at 30 °C. Furthermore, using the same approach and eq 9, we derived the bending rigidity of DMPC/Chol mixture simulated at 30% Chol and at 30 °C (these simulations were reported and analyzed in ref 41) and found K_C^{eff} to be 30 k_BT, again in agreement with Nagle's experimental values.

Table 2. Effective Monolayer Bending Rigidities, K_C^{eff}, for the Simulated Mixtures Calculated Using Eq 9

mixture	K_C^{eff} (k_BT)
SM/Chol 5%	30
SM/Chol 15%	24
SM/Chol 30%	29
SM/Chol 40%	30
DOPC/Chol 10%	9
DOPC/Chol 30%	9

dx.doi.org/10.1021/jp3122006 | J. Phys. Chem. B 2013, 117, 2411−2421

Taken together, the results indicate that the simple model presented in eq 9 closely describes the average bending rigidity of mixed lipid/cholesterol membranes in both liquid ordered and fluid states.

Interestingly, our discussion of the tilt and splay contributions to membrane elasticity are resonant with other molecular level descriptors of membrane organization. For example, Róg et al.[7576] showed that the number of neighbor contacts correlates with the tilt angle. It is reasonable to expect that the derived tilt and splay moduli are good measures of these types of descriptors, too.

At this point the question still remains: what are the molecular mechanistic origins for the differential effect of cholesterol on the elastic properties of membranes composed of saturated versus unsaturated lipids? Our results address this question from the perspective of cholesterol tilt. We have shown quantitatively, in earlier work and again here, that when mixed with saturated lipids, cholesterol molecules create a strong orientational aligning field inside the membrane. The emergence of the aligning field is due to the tendency of Chol molecules to undergo a transition from "lying down" to "standing up" conformation upon increasing concentration. This orientational field aligns not only Chols but also hydrocarbon tails of neighboring lipids. One consequence of this strong alignment is the finding that tilt moduli for Chol and lipid molecules are very similar in the liquid ordered state. In the present work we show, in addition, that the aligning field of cholesterol molecules affects also the splay deformation mode. Thus, the energy cost of creating a splay distortion between a pair of Chol molecules, a pair of lipid tails, or Chol/lipid tail pairs in the liquid ordered state is substantial. In contrast, in the fluid phase, the energy required to induce splay deformation not only is significantly lower compared to that in the L_o phase but also is different for Chol/Chol, lipid/lipid, and Chol/lipid pairs. Stated differently, in liquid-ordered membranes the splay of Chol/Chol, lipid/lipid, and Chol/lipid pairs is highly correlated with each other due to the strong aligning field of Chol molecules in these bilayers. In the fluid L_α phase, on the other hand, this aligning field is not as significant. Consequently, the energy cost of splay deformation is much lower, leading to relatively low bending rigidity for fluid membranes such as DOPC/Chol binary mixtures.

To summarize, our results underscore the splay modulus χ_{12} as a quantitative measure for the bending elastic properties of liquid-ordered membranes and forms a mechanistic link between cholesterol tilt and bending rigidity of lipid bilayers.

CONCLUDING REMARKS

Cholesterol plays a major role in modulating the mechanical properties of lipid membranes in vivo and in vitro. These properties, in turn, are recognized as important for the proper structure and function of biomacromolecules embedded in the membrane. It is well established that cholesterol and lipid alignment in the membrane, as gauged for example by membrane thickness, sensitively depends on the type of lipid in the mixture as well as on sterol content. Importantly, the resulting state (phase) of membranes dictates its mechanical properties. Taken together, cholesterol and lipid tilt degrees of freedom are implicated as determinants of the mixed membrane's elastic properties. To help determine how sterols impact these membrane properties at the molecular level, we have been quantifying the tilt degree of freedom in MD simulations of mixed lipid-cholesterol membranes. By following the fluctuations in tilt and splay in the ensemble, we were able to estimate the contributions of these modes to the response of membranes to elastic deformations.

Using this strategy, we have quantitatively traced the significant differences between saturated and unsaturated lipid mixtures to differences in the degree of cholesterol and lipid alignment in the corresponding membranes. We find that tilt and splay modes have a major contribution to the overall elasticity of the mixed lipid membrane. In fact, these two contributions alone can account for all the observed differences between SM-Chol and DOPC-Chol membrane elasticities. These findings underscore the importance of tilt and splay moduli, derived from simulations with relative computational ease, as useful metrics for quantitatively characterizing the mechanical properties of mixed lipid-cholesterol bilayers.

AUTHOR INFORMATION

Corresponding Author

*(G.K.) E-mail: gek2009@med.cornell.edu. Phone: 212-746-6539. Fax: 212-746-6226. (D.H.) E-mail: daniel@fh.huji.ac.il. Phone: 972-2-6585484. Fax: 972-2-6513742.

Notes

The authors declare no competing financial interest.

ACKNOWLEDGMENTS

We thank Harel Weinstein for insightful discussions and Niklaus Johner and Sayan Mondal for their critical reading of the manuscript. G.K. is supported by HRH Prince Alwaleed Bin Talal Bin Abdulaziz Alsaud Institute of Computational Biomedicine at Weill Medical College of Cornell University. D.H. acknowledges support from the Stephanie Gross intramural fund. Computational resources of the David A. Cofrin Center for Biomedical Information in the HRH Prince Alwaleed Bin Talal Bin Abdulaziz Alsaud Institute for Computational Biomedicine are also gratefully acknowledged. The Fritz Haber Center is supported by the Minerva Foundation, Munich, Germany.

REFERENCES

(1) Pan, J.; Tristram-Nagle, S.; Nagle, J. F. *Phys. Rev. E: Stat., Nonlinear, Soft Matter Phys.* **2009**, *80*, 021931.
(2) Pan, J. J.; Mills, T. T.; Tristram-Nagle, S.; Nagle, J. F. *Phys. Rev. Lett.* **2008**, 100.
(3) Mouritsen, O. G.; Zuckermann, M. J. *Lipids* **2004**, *39*, 1101.
(4) Veatch, S. L. *Semin Cell Dev. Biol.* **2007**, *18*, 573.
(5) Marsh, D. *Biochim. Biophys. Acta* **2009**, *1788*, 2114.
(6) Elson, E. L.; Fried, E.; Dolbow, J. E.; Genin, G. M. *Annu. Rev. Biophys.* **2010**, *39*, 207.
(7) Korade, Z.; Kenworthy, A. K. *Neuropharmacology* **2008**, *55*, 1265.
(8) Marsan, M. P.; Muller, I.; Ramos, C.; Rodriguez, F.; Dufourc, E. J.; Czaplicki, J.; Milon, A. *Biophys. J.* **1999**, *76*, 351.
(9) Pasenkiewicz-Gierula, M.; Rog, T.; Kitamura, K.; Kusumi, A. *Biophys. J.* **2000**, *78*, 1376.
(10) Rog, T.; Pasenkiewicz-Gierula, M.; Vattulainen, I.; Karttunen, M. *Biochim. Biophys. Acta* **2009**, *1788*, 97.
(11) Aittoniemi, J.; Rog, T.; Niemela, P.; Pasenkiewicz-Gierula, M.; Karttunen, M.; Vattulainen, I. *J. Phys. Chem. B* **2006**, *110*, 25562.
(12) Smondyrev, A. M.; Berkowitz, M. L. *Biophys. J.* **2001**, *80*, 1649.
(13) Czub, J.; Baginski, M. *Biophys. J.* **2006**, *90*, 2368.
(14) Douliez, J. P.; Leonard, A.; Dufourc, E. J. *Biophys. J.* **1995**, *68*, 1727.
(15) Urbina, J. A.; Pekerar, S.; Le, H. B.; Patterson, J.; Montez, B.; Oldfield, E. *Biochim. Biophys. Acta* **1995**, *1238*, 163.
(16) Miao, L.; Nielsen, M.; Thewalt, J.; Ipsen, J. H.; Bloom, M.; Zuckermann, M. J.; Mouritsen, O. G. *Biophys. J.* **2002**, *82*, 1429.

(17) Sankaram, M. B.; Thompson, T. E. *Proc. Natl. Acad. Sci. U.S.A.* **1991**, *88*, 8686.
(18) Subramaniam, S. M., H.M. *J. Phys. Chem.* **1986**, *91*, 1715.
(19) Khelashvili, G.; Pabst, G.; Harries, D. *J. Phys. Chem. B* **2010**, *114*, 7524.
(20) Pandit, S. A.; Bostick, D.; Berkowitz, M. L. *Biophys. J.* **2004**, *86*, 1345.
(21) Pandit, S. A.; Chiu, S. W.; Jakobsson, E.; Grama, A.; Scott, H. L. *Langmuir* **2008**, *24*, 6858.
(22) Pandit, S. A.; Jakobsson, E.; Scott, H. L. *Biophys. J.* **2004**, *87*, 3312.
(23) Mallikarjunaiah, K. J.; Leftin, A.; Kinnun, J. J.; Justice, M. J.; Rogozea, A. L.; Petrache, H. I.; Brown, M. F. *Biophys. J.* **2011**, *100*, 98.
(24) de Meyer, F.; Smit, B. *Proc. Natl. Acad. Sci. U.S.A.* **2009**, *106*, 3654.
(25) Wydro, P.; Knapczyk, S.; Lapczynska, M. *Langmuir* **2011**, *27*, 5433.
(26) Mcmullen, T. P. W.; Mcelhaney, R. N. *Biochim. Biophys. Acta, Biomembr.* **1995**, *1234*, 90.
(27) Vist, M. R.; Davis, J. H. *Biochemistry* **1990**, *29*, 451.
(28) Huang, T. H.; Lee, C. W. B.; Dasgupta, S. K.; Blume, A.; Griffin, R. G. *Biochemistry* **1993**, *32*, 13277.
(29) Gracia, R. S.; Bezlyepkina, N.; Knorr, R. L.; Lipowsky, R.; Dimova, R. *Soft Matter* **2010**, *6*, 1472.
(30) Simons, K.; Ikonen, E. *Nature* **1997**, *387*, 569.
(31) Simons, K.; Ikonen, E. *Science* **2000**, *290*, 1721.
(32) Simons, K.; Vaz, W. L. *Annu. Rev. Biophys. Biomol. Struct.* **2004**, *33*, 269.
(33) Lingwood, D.; Simons, K. *Science* **2010**, *327*, 46.
(34) Simons, K.; Gerl, M. J. *Nat. Rev. Mol. Cell Biol.* **2010**, *11*, 688.
(35) May, S.; Kozlovsky, Y.; Ben-Shaul, A.; Kozlov, M. M. *Eur. Phys. J. E* **2004**, *14*, 299.
(36) Fosnaric, M.; Iglic, A.; May, S. *Phys. Rev. E: Stat., Nonlinear, Soft Matter Phys.* **2006**, *74*, 051503.
(37) Kozlovsky, Y.; Kozlov, M. M. *Biophys. J.* **2002**, *82*, 882.
(38) Harroun, T. A.; Katsaras, J.; Wassall, S. R. *Biochemistry* **2008**, *47*, 7090.
(39) Kucerka, N.; Perlmutter, J. D.; Pan, J.; Tristram-Nagle, S.; Katsaras, J.; Sachs, J. N. *Biophys. J.* **2008**, *95*, 2792.
(40) Khelashvili, G.; Mondal, S.; Andersen, O. S.; Weinstein, H. *J. Phys. Chem. B* **2010**, *114*, 12046.
(41) Khelashvili, G.; Rappolt, M.; Chiu, S.-W.; Pabst, G.; Harries, D. *Soft Matter* **2011**, *7*, 10299.
(42) Khelashvili, G.; Harries, D. *Chem. Phys. Lipids* **2013**, DOI: 10.1016/j.chemphyslip.2012.12.006.
(43) Marsh, D. *Biochim. Biophys. Acta* **2010**, *1798*, 688.
(44) Leonenko, Z. V.; Finot, E.; Ma, H.; Dahms, T. E.; Cramb, D. T. *Biophys. J.* **2004**, *86*, 3783.
(45) Hess, B.; Kutzner, C.; van der Spoel, D.; Lindahl, E. *J. Chem. Theory Comput.* **2008**, *4*, 435.
(46) Chiu, S. W.; Pandit, S. A.; Scott, H. L.; Jakobsson, E. *J. Phys. Chem. B* **2009**, *113*, 2748.
(47) Hess, B.; Bekker, H.; Berendsen, H. J. C.; Fraaije, J. G. E. M. *J. Comput. Chem.* **1997**, *18*, 1463.
(48) Essmann, U.; Perera, L.; Berkowitz, M. L.; Darden, T.; Lee, H.; Pedersen, L. G. *J. Chem. Phys.* **1995**, *103*, 8577.
(49) Nose, S.; Klein, M. L. *J. Chem. Phys.* **1983**, *78*, 6928.
(50) Parrinello, M.; Rahman, A. *J. Appl. Phys.* **1981**, *52*, 7182.
(51) Evans, D. J.; Holian, B. L. *J. Chem. Phys.* **1985**, *83*, 4069.
(52) Kessel, A.; Ben-Tal, N.; May, S. *Biophys. J.* **2001**, *81*, 643.
(53) de Almeida, R. F.; Fedorov, A.; Prieto, M. *Biophys. J.* **2003**, *85*, 2406.
(54) Kusumi, A.; Pasenkiewicz-Gierula, M. *Biochemistry* **1988**, *27*, 4407.
(55) Pasenkiewicz-Gierula, M.; Subczynski, W. K.; Kusumi, A. *Biochemistry* **1990**, *29*, 4059.
(56) Guo, W.; Kurze, V.; Huber, T.; Afdhal, N. H.; Beyer, K.; Hamilton, J. A. *Biophys. J.* **2002**, *83*, 1465.
(57) Kramer, D.; Benshaul, A.; Chen, Z. Y.; Gelbart, W. M. *J. Chem. Phys.* **1992**, *96*, 2236.
(58) Martinez-Seara, H.; Rog, T.; Karttunen, M.; Vattulainen, I.; Reigada, R. *PLoS One* **2010**, *5*, e11162.
(59) Zhang, Z.; Lu, L.; Berkowitz, M. L. *J. Phys. Chem. B* **2008**, *112*, 3807.
(60) Bennett, W. F.; MacCallum, J. L.; Hinner, M. J.; Marrink, S. J.; Tieleman, D. P. *J. Am. Chem. Soc.* **2009**, *131*, 12714.
(61) Olsen, B. N.; Schlesinger, P. H.; Baker, N. A. *J. Am. Chem. Soc.* **2009**, *131*, 4854.
(62) Helfrich, W. *Z. Naturforsch. C* **1973**, *28*, 693.
(63) Canham, P. B. *J. Theor. Biol.* **1970**, *26*, 61.
(64) Evans, E. A. *Biophys. J.* **1974**, *14*, 923.
(65) Watson, M. C.; Penev, E. S.; Welch, P. M.; Brown, F. L. *J. Chem. Phys.* **2011**, *135*, 244701.
(66) Khelashvili, G. A.; Scott, H. L. *J. Chem. Phys.* **2004**, *120*, 9841.
(67) Chiu, S. W.; Vasudevan, S.; Jakobsson, E.; Mashl, R. J.; Scott, H. L. *Biophys. J.* **2003**, *85*, 3624.
(68) Pandit, S. A.; Vasudevan, S.; Chiu, S. W.; Mashl, R. J.; Jakobsson, E.; Scott, H. L. *Biophys. J.* **2004**, *87*, 1092.
(69) Chiantia, S.; London, E. *Biophys. J.* **2012**, *103*, 2311.
(70) Safran, S. A.; Pincus, P. A.; Andelman, D.; MacKintosh, F. C. *Phys. Rev. A* **1991**, *43*, 1071.
(71) Kozlov, M. M.; Helfrich, W. *Langmuir* **1992**, *8*, 2792.
(72) Porte, G.; Ligoure, C. *J. Chem. Phys.* **1995**, *102*, 4290.
(73) May, S.; Ben-Shaul, A. *J. Chem. Phys.* **1995**, *103*, 3839.
(74) Illya, G.; Lipowsky, R.; Shillcock, J. C. *J. Chem. Phys.* **2006**, *125*, 114710.
(75) Rog, T.; Pasenkiewicz-Gierula, M.; Vattulainen, I.; Karttunen, M. *Biophys. J.* **2007**, *92*, 3346.
(76) Rog, T.; Vattulainen, I.; Jansen, M.; Ikonen, E.; Karttunen, M. *J. Chem. Phys.* **2008**, *129*, 154508.

NOTE ADDED AFTER ASAP PUBLICATION

This paper was published ASAP on January 30, 2013. A reference was added (ref 42), and also, the author list in ref 41 was corrected. The paper was reposted on February 20, 2013.